EFDA–JET–PR(07)47

G. Ambrosino, M. Ariola, G De Tommasi, A. Pironti, F. Sartori, E. Joffrin,
F. Villone and JET EFDA contributors

Plasma Strike-Points Sweeping on JET Tokamak with the eXtreme Shape Controller

"This document is intended for publication in the open literature. It is made available on the understanding that it may not be further circulated and extracts or references may not be published prior to publication of the original when applicable, or without the consent of the Publications Officer, EFDA, Culham Science Centre, Abingdon, Oxon, OX14 3DB, UK."

"Enquiries about Copyright and reproduction should be addressed to the Publications Officer, EFDA, Culham Science Centre, Abingdon, Oxon, OX14 3DB, UK."

Plasma Strike-Points Sweeping on JET Tokamak with the eXtreme Shape Controller

G. Ambrosino[1], M. Ariola[2], G De Tommasi[1], A. Pironti[1], F. Sartori[3], E. Joffrin[4,5], F. Villone[6] and JET EFDA contributors*

JET-EFDA, Culham Science Centre, OX14 3DB, Abingdon, UK

[1]Associazione Euratom-ENEA-CREATE, Universit'a di Napoli Federico II, via Claudio 21, 80125, Napoli, Italy
[2]Associazione Euratom-ENEA-CREATE, Universit'a di Napoli Parthenope, via Medina 40, 80133 Napoli, Italy
[3]EURATOM-UKAEA Fusion Association, Culham Science Centre, Abingdon, OX14 3EA
[4]EFDA-JET-CSU, Culham Science Centre, Abingdon, Oxfordshire OX14 3DB
[5]Association EURATOM-CEA, DSM-DRFC, CEA Cadarache, 13108 St Paul lez Durance, France
[6]Associazione Euratom-ENEA-CREATE, Universit'a di Cassino, via Di Biasio 43, 03043, Cassino, Italy
** See annex of M.L. Watkins et al, "Overview of JET Results ",*
(Proc. 21 st IAEA Fusion Energy Conference, Chengdu, China (2006)).

Preprint of Paper to be submitted for publication in
IEEE Transactions on Plasma Science

ABSTRACT

The high energy ionized particles collected by the divertor structures in a tokamak reactor cause a localized thermal load around the strike-points, which are the intersections of the separatrix with the divertor tiles. To spread on a larger region this thermal load it is convenient to resort to a *sweeping*, i.e. a periodical movement of the strike points. This paper introduces the new model-based sweeping algorithm recently implemented on the JET tokamak, within the eXtreme Shape Controller architecture.

1. INTRODUCTION

Tokamaks [1] are the most promising confinement devices in the field of thermonuclear fusion. During tokamak operation different types of high energy ionized particles are produced and leave the plasma after the confinement time. Among them there is ionized helium, which is the byproduct of the fusion reaction, and the so called “impurities”, i.e. heavy metals present in the vacuum chamber, carbon, oxygen, and noble gases, such as neon and argon, which are sometimes injected into the reactor to create the radiating mantle [2].

All these ionized particles must be removed from the vacuum chamber to prevent them to interfere with the subsequent fusion reactions. The *divertor* structures shown in Fig.1, collect all the escaping high energy particles and remove them from the reactor. In fact, when the exhaust particles escape from the plasma, they enter in the *Scrape-Off Layer* (SOL) region, which is the region just outside the last closed flux surface inside the vacuum chamber, called *separatrix* (see Fig.1). Particles in the SOL are still ionized, thus they continue to follow the magnetic field lines, which terminate on the interior plasma-facing structures in the divertor region.

The exhaust particles collected in the divertor region cause a localized thermal load around the *strike-points*, i.e. the intersections of the separatrix with the divertor (see Fig.1). To spread on a larger region this thermal load it is convenient to resort to a periodical movement of the strike-points called *sweeping*. The accurate control of plasma shape inside the vacuum chamber plays an essential role to obtain the values of elongation and triangularity needed in high-performance plasmas [3]. In principle the strike-point sweeping should cause only a minor variation in the desired shape. It follows that the strikepoints sweeping algorithm should be integrated in the plasma shape control system in order to perform thermal load spread without affecting too much the plasma shape.

The standard sweeping strategy adopted at Joint European Torus (JET) tokamak [4] is implemented within the *Shape Controller* (SC) architecture [5]. In this case the strike-point sweeping is performed with a 4Hz triangular reference for either the currents in the divertor coils $D2$ and $D3$ shown in Fig.2. Since the divertor coils circuits have a 10 Hz bandwidth when driven in current control mode, the sweeping frequency has been chosen equal to 4 Hz so to reproduce a triangular reference up to the third harmonic. This standard approach suffers from the inconvenience that the movement of the strikepoints causes, to a certain amount, a 4 Hz oscillation of the overall shape.

In order to avoid these shape oscillations it is possible to design the sweeping currents waveforms

adopting a model-Divertor structure is the gray area outside the separatrix, while the *strike-points* are the intersections between the separatrix and the divertor structure. based approach [6]. This paper introduces a new modelbased sweeping strategy, which has been implemented and effectively used on the JET tokamak within the eXtreme Shape Controller architecture (XSC) [7]. The results achieved during the 2006-07 JET experimental campaign are presented as well.

The paper is divided as follows. A brief discussion of plasma modeling for the shape control in tokamaks is given in Section II, together with a short introduction to the XSC. Section III deals with the sweeping algorithm implemented on the JET tokamak in the XSC architecture. Some experimental results are presented in Section IV, while a conclusive discussion is given in Section V.

2. PLASMA MODELING AND SHAPE CONTROL

This section introduces the model for plasma shape control exploited in this paper together with the XSC control algorithm. A survey on plasma modeling for shape control can be found in [8], while a complete description of the XSC can be found in [7].

A. PLASMA LINEAR MODEL

The plasma linearized state space model [9] presented in this paragraph describes the behavior of the plasma shape around a given equilibrium, which is specified in terms of nominal values of plasma current I_{pN}, Poloidal Field (PF) coils[1] currents $\mathbf{I}_{PFN}$, poloidal beta β_{pN}, and internal inductance l_{iN}[2].

In particular it relates the variations of n_G plasma shape geometrical descriptors around a given equilibrium to the variation of the currents in n_{PF} PF coils, and to the variations of β_p and l_i, as follows:

$$\delta\dot{\mathbf{x}}(t) = \mathbf{A}\delta\mathbf{x}(t) + \mathbf{B}\delta\mathbf{u}(t) + \mathbf{E}\delta\dot{\mathbf{w}}(t), \tag{1a}$$

$$\delta\mathbf{g}(t) = \mathbf{C}\ \mathrm{d}\mathbf{I}_{PF}(t) + \mathbf{F}\delta\mathbf{w}(t), \tag{1b}$$

where:

- **A, B, E, C** and **F** are the model matrices;
- $\delta\mathbf{x}(t) = [\delta\mathbf{I}_{PF}^{\mathrm{T}}(t)\ \delta I_p(t)]^{\mathrm{T}} \in \mathbb{R}^{(n_{PF}+1)}$ is the state space vector, which includes the variations of the currents in the PF circuits, and of the plasma current[3];
- $\delta\mathbf{u}(t) = [\delta\mathbf{U}_{PF}(t)\ 0]^{\mathrm{T}} \in \mathbb{R}^{(n_{PF}+1)}$ are the input voltages variations;
- $\delta\mathbf{w}(t) = [\delta\beta_p(t)\ \delta I_i(t)]^{\mathrm{T}} \in \mathbb{R}^2$ are the β_p and l_i variations;
- $\delta\mathbf{g}(t) \in \mathbb{R}^{n_G}$ are the plasma shape descriptors variations, which include a number of gaps – i.e. distances between the plasma separatrix the reactor vacuum chamber – the X-point and the strike-points positions (see Fig.3).

[1] *A description of the JET Poloidal Field Coils system can be found in [5], and it is here omitted for sake of brevity.*
[2] *$\beta p(t)$ and $l_i(t)$ measures the plasma internal distributions of pressure and current respectively.*
[3] *The superscript T denotes the vector/matrix transpose.*

In the following the effects of the plasma profile parameters d$b_p(t)$ and d$l_i(t)$, which can be regarded as disturbances, will be neglected.

B. EXTREME SHAPE CONTROLLER (XSC)

The XSC controls the whole plasma shape specified as a set of n_G geometrical descriptors, calculating the n_{PF} PF coil current references (typically $n_G = 32$, and $n_{PF} = 8$).

In particular its design is based on the **C** matrix o model (1a)–(1b). Note that the plasma is a non-right-invertible plant, i.e. the number of independent control variables is less than the number of outputs to regulate, i.e. $n_{PF} < n_G$. For such a plant it is not possible to track a generic set of references with zero steady-state error. Given a generic set of references, the best performance that can be achieved in steady-state is to control to zero the error on n_{PF} linear combinations of geometrical descriptors. Control to zero such an error is equivalent to minimize the following steady-state performance index (see [10])

$$J = \lim_{t \to +\infty} (\delta g_{ref} - \delta g(t))^T (\delta g_{ref} - \delta g(t)), \tag{2}$$

where $\delta \mathbf{g}_{ref}$ are constant references to the geometrical descriptors.

Minimization of (2) can be attained using the Singular Value Decomposition (SVD) of the **C** matrix:

$$\mathbf{C} = \mathbf{U}\,\mathbf{S}\,\mathbf{V}^{\mathrm{T}},$$

where the matrix **S** contains the singular values, **U** and **V** are unitary matrices, and computing the PF currents references as:

$$I_{PF_{ref}}(t) = \mathbf{V}\,\mathbf{S}^{-1}\,\mathbf{U}^{\mathrm{T}}\,(\delta \mathbf{g}_{ref} - \delta \mathbf{g}(t)) + \mathbf{I}_{PF_N}.$$

To extend this approach to the dynamical case the PF current references are computing using n_{PF} Proportional-Integral regulators (PIs). In particular the output of the i-th PI is given by:

$$\begin{aligned} I_{PF}(t) &= k_P \mathrm{v}_i^{\mathrm{T}} \mathrm{S}^{-1} \mathrm{U}^{\mathrm{T}} (\delta g_{ref}(t)) - \delta g(t)) + \\ &+ k_I \int_0^t \mathrm{v}_i^{\mathrm{T}} \mathrm{S}^{-1} \mathrm{U}^{\mathrm{T}} (\delta g_{ref}(\alpha) - \delta g(\alpha)) d\alpha + I_{PFN_i}, \end{aligned} \tag{3}$$

where k_P and k_I are the PI gains, and $\mathbf{v}_i^{\mathrm{T}}$ is the i-th row vector of matrix **V**.

A more sophisticated version of the XSC has been implemented introducing weight matrices both for the geometrical descriptors and for the PF coil currents. The reason for this lies in the fact that there are some regions of the plasma boundary where more tight requirements are requested, for instance for the antenna power coupling. Also, the PF coil currents available for feedback purposes differ significantly from coil to coil and among different scenarios.

3. STRIKE-POINT SWEEPING WITH THE XSC

The modified XSC architecture adopted on the JET tokamak to perform the strike-point sweeping is presented in this section, together with the algorithm adopted to compute the sweeping waveforms.

A. CONTROLLER ARCHITECTURE

The sweeping problem concerns how to let oscillate the plasma boundary between two different configurations named A and *B*, following a given waveform at a given frequency. As far as the strike-points sweeping problem is concerned, the configurations *A* and *B* differ significantly only in the bottom part of the plasma (see Fig.4).

In principle the sweeping could be obtained by using the XSC, and choosing the shape references according to the desired waveforms. Unfortunately at JET this approach cannot be pursued, because the required sweeping frequency (4Hz) is just outside the closed loop system bandwidth guaranteed by the XSC. The closed loop frequency behavior of the XSC is limited by the speed of the slowest power supply of the PF coils system.

To overcome this problem the XSC architecture has been modified as shown in Fig.5. In particular the XSC is composed by two subsystems: the *Shape Controller* and the *PF Currents Controller* [7]. The former, whose input is the plasma shape tracking error, computes the PF coils current references (3). These current references are then tracked by the latter block, which computes the voltages to be applied to the PF circuits. The PF Currents Controller performs the tracking of the PF currents as fast as possible according to the PF circuit power supplies characteristics.

In order to perform the strike-points sweeping with the XSC, two additional references $\mathbf{I}_{sw}(t)$ and $\mathbf{G}_{sw}(t)$ have been added at the input of the Shape Controller and the PF Currents Controller subsystems, respectively. Since only the currents in the divertor coils *D*1-*D*4 are used to perform the sweeping, the feedforward PF currents vector $\mathbf{I}_{sw}(t)$ can be partitioned as follows

$$\mathbf{I}_{sw}(t) = [\mathbf{0}\ \mathbf{I}^{T}_{div}(t)]^{T} ,$$

with $\mathbf{0} \in \mathbb{R}^{n_{PF}-4}$, and $\mathbf{I}_{div}(t) \in \mathbb{R}^{4}$. The divertor currents waveforms $\mathbf{I}_{div}(t)$ are then computed so to obtain the desired sweeping movement, as it will be shown in Section III-B.

The additional shape references $\mathbf{G}_{sw}(t)$ are chosen so to blind the XSC with respect to sweeping movement, thus they allow to avoid shape oscillations induced by the strike-points sweeping. $\mathbf{G}_{sw}(t)$ is computed multiplying $\mathbf{I}_{sw}(t)$ by the output matrix $\mathbf{C}$. Let

$$\mathbf{C} = [\tilde{\mathbf{C}}\ \ \mathbf{C}_{div}] ,$$

where $\mathbf{C}_{div} \in \mathbb{R}^{n_G \times 4}$ are the columns of the output matrix which correspond to the currents in the four divertor coils. It follows that the vector $\mathbf{G}_{sw}(t)$ can be computed as

$$\mathbf{G}_{sw}(t) = \mathbf{C}_{div}\,\mathbf{I}_{div}(t) .$$

B. SWEEPING ALGORITHM

The evaluation of the currents vector $\mathbf{I}_{\text{div}}(t)$ is performed exploiting the model output equation (1b). These divertor currents variations move the plasma from the nominal shape *N*, to the desired configurations *A* and *B* (see Fig.4). $\mathbf{I}_{\text{div}}(t)$ is computed off-line via the static optimization procedure introduced in this section.

Let consider the following partition of the $\mathbf{C}_{\text{div}}$ matrix

$$C_{\text{div}}=\begin{bmatrix} C_{\text{div}}^{\uparrow} \\ C_{\text{div}}^{\downarrow} \end{bmatrix},$$

where $\mathbf{C}^{\downarrow}_{\text{div}}$ are the rows corresponding to the geometrical descriptors of the *bottom part* of the plasma, i.e. the descriptors shown in the shaded area of Fig.3. This set includes the strikepoints, the X-point, and a number of gaps. It follows that the $\mathbf{C}^{\uparrow}_{\text{div}}$ matrix describes the relationship between the currents in the divertor coils and the *upper* plasma shape descriptors, which are the ones not included in the shaded area of Fig.3. Performing the SVD of the $\mathbf{C}^{\uparrow}_{\text{div}}$ we obtain

$$C_{\text{div}}^{\uparrow}=\mathbf{U}^{\uparrow}\mathbf{S}^{\uparrow}\mathbf{V}^{\uparrow T}= \\ =\begin{bmatrix} U_1^{\uparrow} & U_2^{\uparrow} \end{bmatrix}\begin{bmatrix} S_1^{\uparrow} & 0 \\ 0 & S_2^{\uparrow} \end{bmatrix}\begin{bmatrix} V_1^{\uparrow} & V_2^{\uparrow} \end{bmatrix}^{T},$$

where $\mathbf{V}^{\uparrow}_{2} = [\mathbf{v}_2^{(1)}\ \mathbf{v}_2^{(2)}] \in \mathbb{R}^{4\times 2}$ are the two columns of $\mathbf{V}^{\uparrow}$ corresponding to the two smallest singular values of $\mathbf{C}^{\uparrow}_{\text{div}}$.

It follows that $\mathbf{v}_2^{(1)}$ and $\mathbf{v}_2^{(2)}$ represent two divertor currents vectors which negligibly affect the upper part of the plasma shape. Furthermore these two currents combinations allow to effectively modify the bottom part of the plasma shape. In particular the variation of the swept variable obtained by using $\mathbf{v}_2^{(i)}$ is given by

$$\delta g_{swept}^{(i)} = \mathbf{c}_{swept}^{T}\,\mathbf{v}_2^{(i)}, \quad i = 1,2,$$

where $\mathbf{c}^{T}_{\text{swept}}$ is the row of the $\mathbf{C}^{\downarrow}_{\text{div}}$ matrix which corresponds to the swept variable (e.g. the outer strike-point).

In order to minimize the divertor currents needed to obtained a unitary variation of the swept variable the following optimal convex combination can be considered

$$v = \tilde{\alpha}\frac{v_2^{(1)}}{\delta g_{swept}^{(1)}} + (1-\tilde{\alpha})\frac{v_2^{(2)}}{\delta g_{swept}^{(2)}},\ 0 \le \tilde{\alpha} \le 1,$$

with

$$\alpha = \tilde{\arg}\min_{\alpha}\left\| \alpha\frac{v_2^{(1)}}{\delta g_{swept}^{(1)}} + (1-\alpha)\frac{v_2^{(2)}}{\delta g_{swept}^{(2)}} \right\|,\ 0 \le \alpha \le 1.$$

$\|\cdot\|$ denotes the norm of a vector.

Let denote with $\delta g_{sweep}(t)$, $t \in [0, T]$, a period of the sweeping waveform for the swept variable. Then the sweeping vector for the four divertor coils is computed off-line as follows

$$\mathbf{I}_{div}(t) = \delta g_{sweep}(t) \cdot \mathrm{v}, \; t \in [0, T] \; .$$

4. EXPERIMENTAL RESULTS

The validation of the proposed sweeping algorithm has been carried out during the C15-C17 experimental campaigns at JET in 2006-07.

The pulses described hereafter have been performed during the *Stationary hybrid scenario* session, which was aimed to perform long pulses in hybrid regimes [11], [12]. In particular, the toroidal magnetic field B_T was equal to 1.5T, the nominal plasma current was 1.3MA, while the available additional heating powers during the 20s plasma current flat-top was about 10 MW4. The requirement was to spread as much as possible the heating load on the divertor region, moving the strike-points on the tiles between the two extremal configurations shown in Fig.6(c). Figure 6(a) shows the experimental waveforms of both the inner and the outer strike-points, ZSI and RSO respectively (see Fig.3). The sweeping has been performed at 4Hz. Figure 6(b) shows the time behavior of two gaps in the upper part of the plasma. Note that for these gaps the 4Hz oscillations are negligible (~ 1mm). Figure 7 shows the effects of the strike-points sweeping on the temperature of the divertor tiles. In this figure two similar pulses, one without the sweeping (Pulse No: 68409), and one with the sweeping (Pulse No: 68414) are considered. By using the measurements coming from the new infrared camera [13], it is possible to notice that the sweeping allows to reduce the temperature in the region where the two strike-points intersect the divertor structure. The *flat-top* phase is such that the plasma current has reached the target value. At the end of the flat-top, the plasma current starts the *ramp-down* so to terminate the pulse.

CONCLUSION

A new model-based algorithm for the strike-points sweeping in a tokamak reactor has been presented. The proposed algorithm has been implemented within the JET eXtreme Shape Controller architecture, and it allows to perform the strikepoints sweeping without affecting the plasma boundary shape control. Experimental validation of the proposed approach has been successfully achieved during the JET 2006-07 experimental campaign.

The XSC strike-point sweeping algorithm, together with the plasma boundary flux controller [14], could be combined with a plasma controller for future JET high power long pulse operation [15].

ACKNOWLEDGMENTS

The authors would like to thanks the leader of the *XSC Phase II Enhancement Project* Dr. Flavio Crisanti and the members of the CREATE team Prof. Raffaele Albanese and Prof. Massimiliano Mattei. This work has been conducted under the European Fusion Development Agreement, and it has been partially supported by Italian MiUR (PRIN grant #2006094025).

REFERENCES

[1]. J. Wesson, *Tokamas*. Oxford University Press, 2004.

[2]. U. Samm *et al.*, "Radiative edges under control by impurity fluxes," *Plasma Physics and Controller Fusion*, vol. **35**, no. B, pp. B167–B175, December 1993.

[3]. F.G. Rimini *et al.*, "Design and exploitation of advanced Tokamak scenarios with the new extreme shape controller at JET," in *Proceedings of the* 24th *Symposium on Fusion Technology (SOFT 2006)*, Warsaw, Poland, September 2006.

[4]. J. Wesson, *The science of JET*. Abingdon, Oxon: JET Joint Undertaking, 2000.

[5]. F. Sartori, G. De Tommasi, and F. Piccolo, "The Joint European Torus," *IEEE Control Systems Magazine*, vol. **26**, no. 2, pp. 64–78, 2006.

[6]. F. Villone, "A model-based strike point sweeping technique applied to JET,""*Plasma Physics and Controlled Fusion*, vol. **46**, no. 9, pp. 1375–1392, September 2004.

[7]. M. Ariola and A. Pironti,–"The design of the extreme shape controller for the JET tokamak,""*IEEE Control Systems Magazine*, vol. **25**, no. 5, pp. 65–75, 2005.

[8]. G. Ambrosino and R. Albanese, "A survey on modeling and control of current, position and shape of axisymmetric plasmas,""*IEEE Control Systems Magazine*, vol. **26**, no. 5, pp. 76–91, 2005.

[9]. R. Albanese, G. Calabr'o M. Mattei, and F. Villone, "Plasma response models for current, shape and position control at JET,""*Fusion Engineering and Design*, vol. **66–68**, pp. 715–718, 2003.

[10]. G. Ambrosino, M. Ariola, and A. Pironti, "Optimal steady-state control for linear non-right-invertible systems," "*IET Control Theory Applications*, vol. **1**, no. 3, pp. 604–610, May 2007.

[11]. E. Joffrin *et al.*, "Stationary 20 s Hybrid Discharge in JET," in 5th IAEA Technical Meeting on Steady State Operations of Magnetic Fusion *Devices (IAEA SSO 2007)*, Daejeon, Republic of Korea, May 2007.

[12]. F. Villone *et al.*, "Development of 20s long hybrid scenarios on JET," in 34th *EPS Conference on Plasma Physics*, Warsaw, Poland, 2007.

[13]. E. Gauthier *et al.*, "Design of a Wide-Angle Infrared Thermography and Visible View Diagnostic for JET," in 33rd *EPS Conference on Plasma Physics*, Tarragona, Spain, 2005.

[14]. M. Ariola *et al.*, "Integrated plasma shape and boundary flux control on JET tokamak,""*Fusion Science and Technology*, 2007, accepted for pubblication.

[15]. D. Moreau *et al.*, "A Multiple Time Scale Dynamic-Model Approach for Magnetic and Kinetic Profile Control in Advanced Tokamak Scenario," *Nuclear Fusion*, 2007, submitted for pubblication.

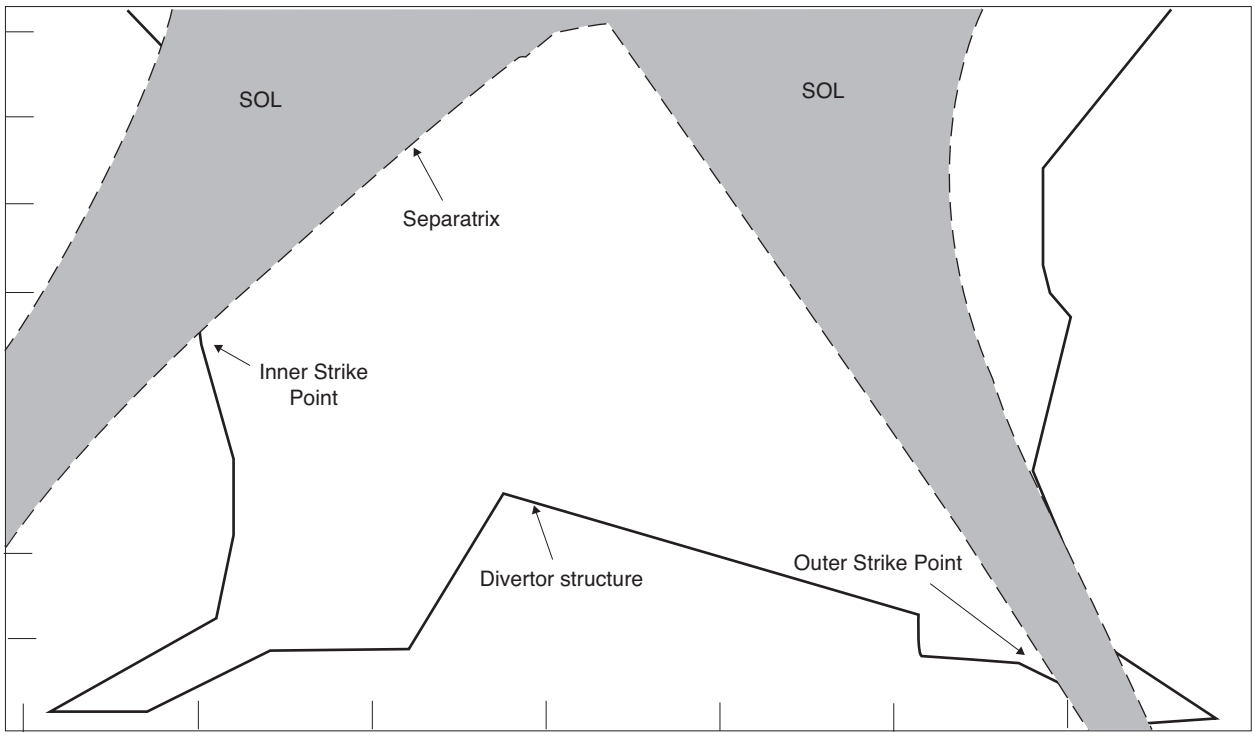

Figure 1: A poloidal cross-section of the divertor zone of the JET tokamak. The Scrape-Off Layer (SOL)

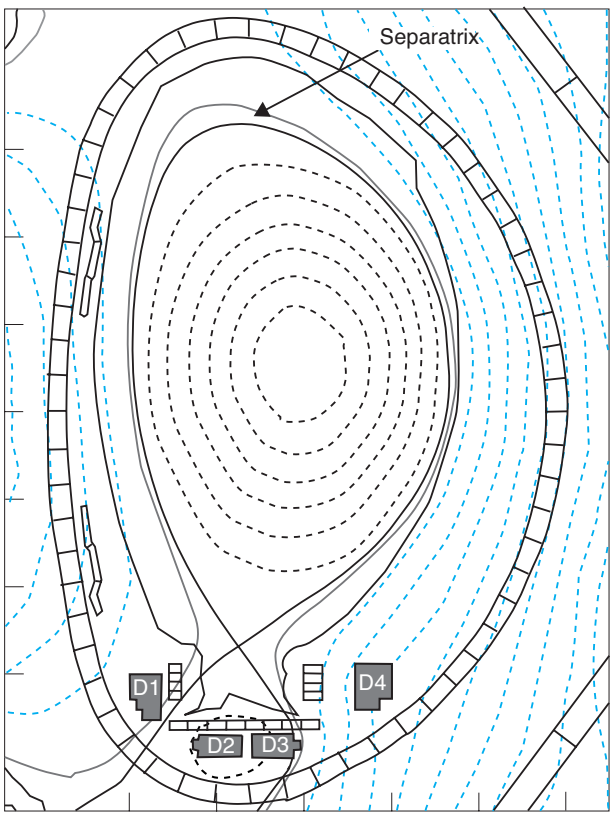

Figure 2: A poloidal cross-section of the JET tokamak. The four divertor coils (D1 to D4) are shown. This poloidal field coils are driven separately each by one power supply.

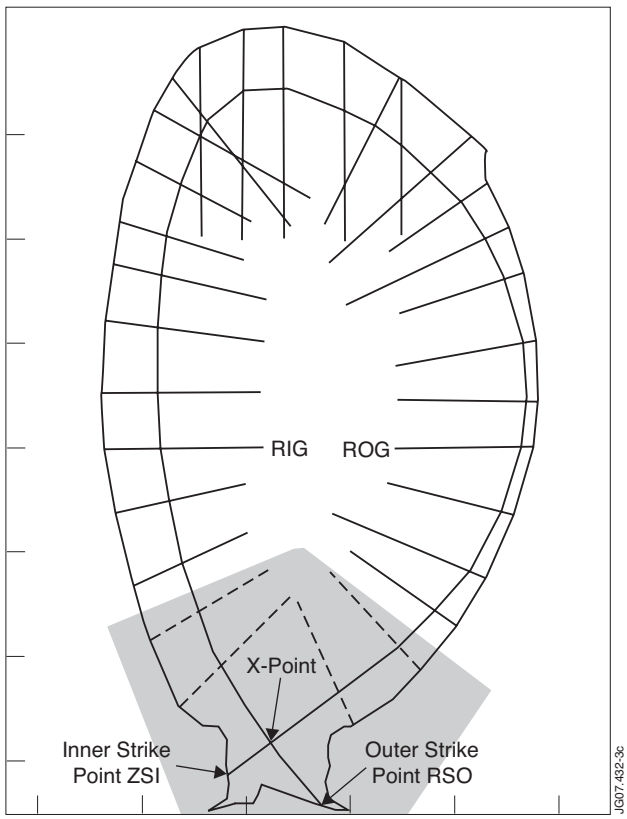

Figure 3: Plasma boundary descriptors. This figure shows the gaps typically controlled by the eXtreme Shape Controller on the JET tokamak, together with the strike-points and the X-point.

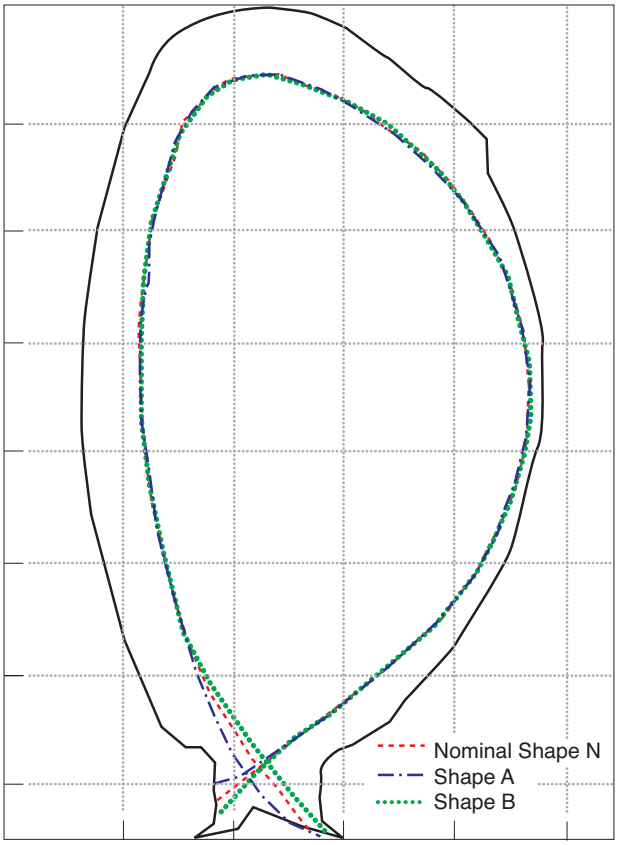

Figure 4: An example of strike-point sweeping. The nominal shape N and the two varied configurations A and B are shown.

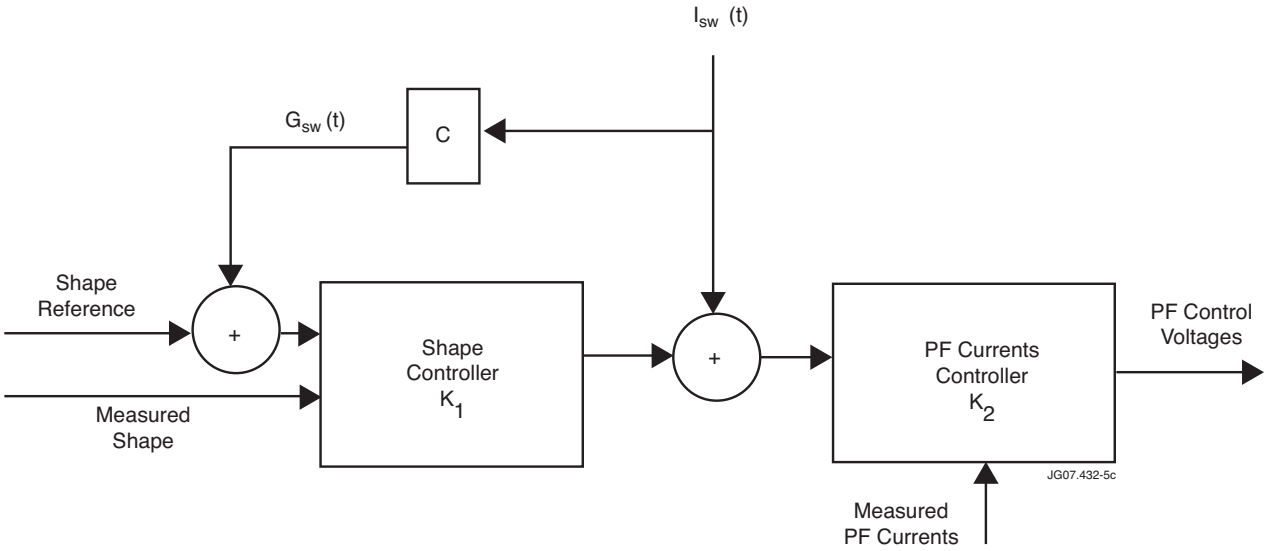

Figure 5. The scheme used to perform the strike-points sweeping at JET with the XSC.

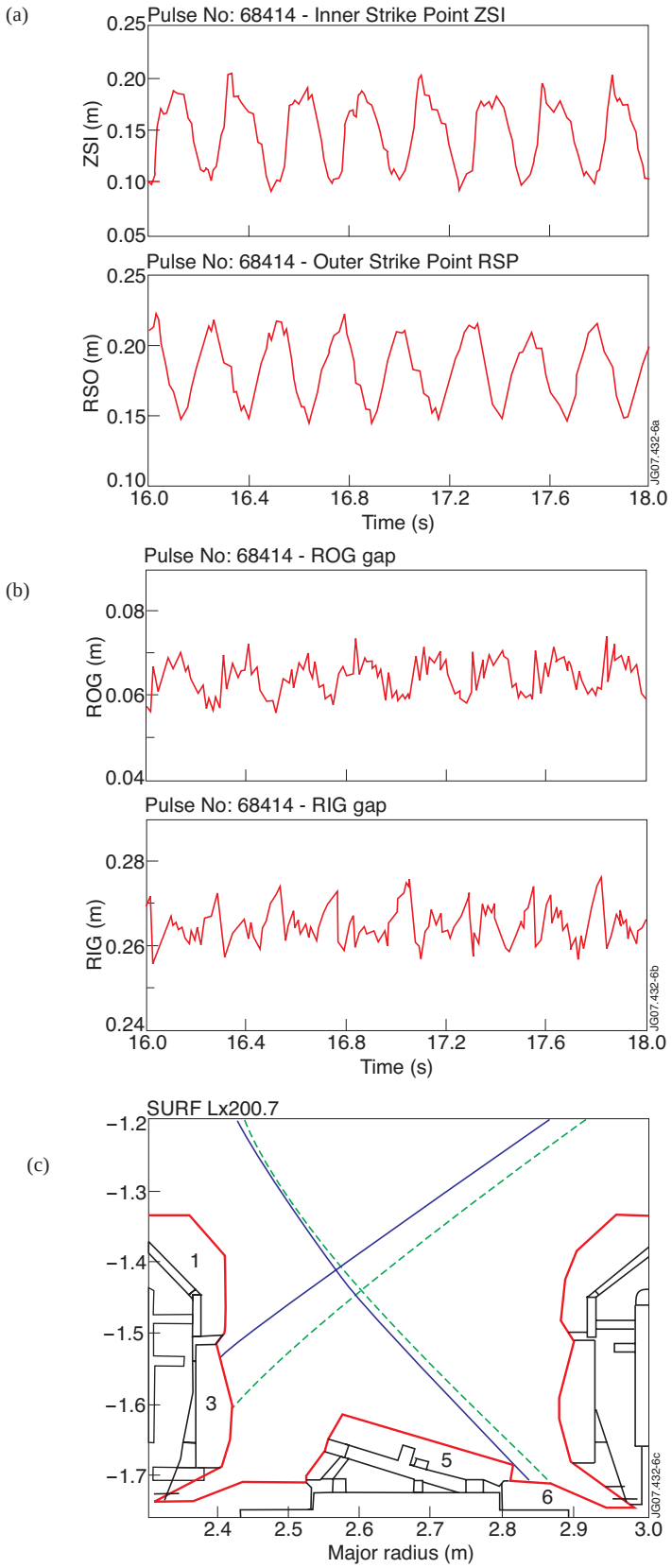

Figure 6: Sweeping experimental results for the JET Pulse No: 68414. (a) Time behavior of the inner (ZSI) and outer (RSO) strike-points. Note that ZSI is measured along the vertical direction, whereas RSO is measured along the radial direction. (b) Time behavior of the radial outer (ROG) and radial inner (RIG) gaps. The positions of these two gaps is shown in Fig.3 (c) Shapes at t = 17.1s and t = 17.2s.

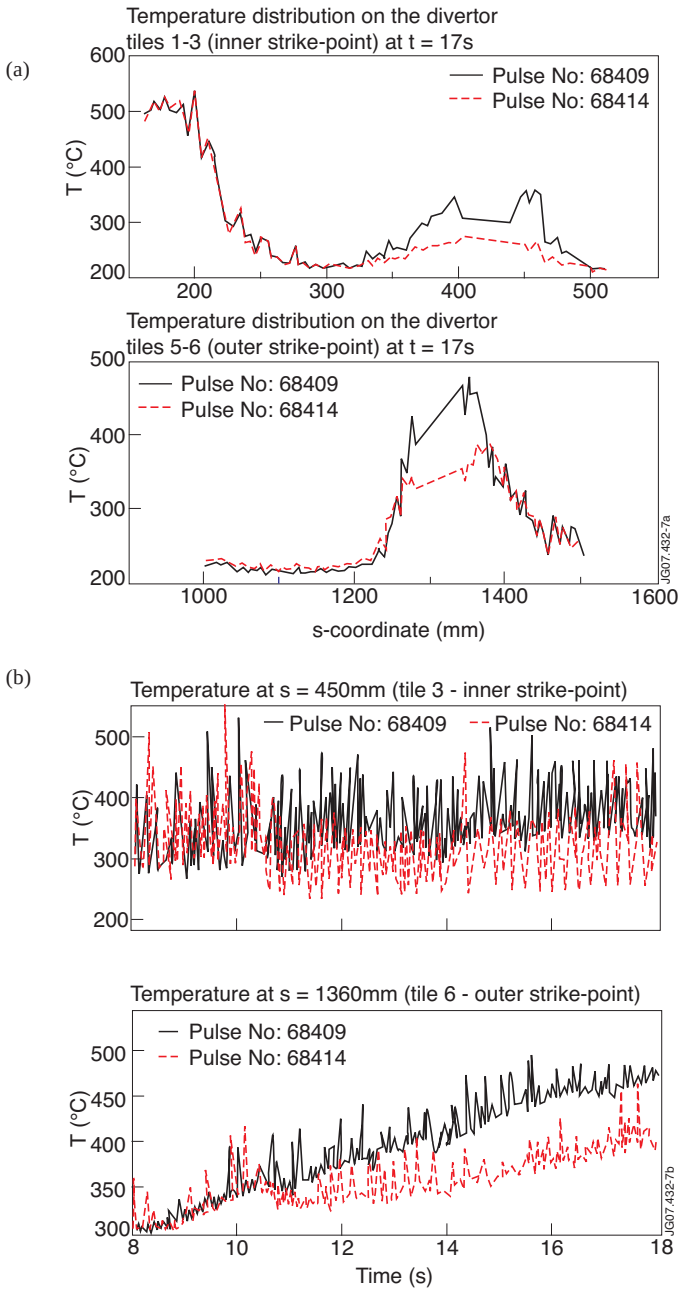

Figure 7: Comparison between the JET Pulse No's: 68409 and 68414. These two pulses have the same plasma parameters and regimes. The only differences is the that the former has been carried out without strike-point sweeping, while during the latter the strike-point sweeping has been performed.(a) Divertor temperature profiles with (Pulse No: 68414) and without (Pulse No: 68409) the sweeping. The s-coordinate is a poloidal coordinate defined along the divertor surface. (b) Time behavior of the divertor temperatures with (Pulse No: 68414) and without (Pulse No: 68409) the sweeping.